Surface Modification and Stabilization of Rubber Materials: Plasma Polymerization and Photografting

BENGT MATTSON* and BENGT STENBERG

Department of Polymer Technology, Royal Institute of Technology, S-100 44 Stockholm, Sweden

SYNOPSIS

Thermooxidative degradation of thick-walled rubber materials is dependent on oxygen diffusion. The oxidative degradation ceases due to a lower permeability of oxygen through the oxidized material formed at the rubber surface. This phenomenon indicates a paradoxical effect of antioxidant loading. Since antioxidants prevent oxidation, antioxidants also prevent the formation of the protective oxidized layer. This paper suggests and explores an attempt to stabilize polymer materials using surface-modification techniques in order to form an oxygen permeation barrier at the surface. Two techniques, plasma polymerization and photografting, suitable for such surface modifications are described. © 1993 John Wiley & Sons, Inc.

INTRODUCTION

Organic compounds are susceptible to attack by molecular oxygen.[1-3] This reaction is often referred to as autoxidation.[4,5] The well-known autoxidation scheme for hydrocarbon materials[6,7] is reported in Figure 1, and the products finally produced in the oxidation[8-10] are shown in Figure 2. The major products are carbonyl compounds, e.g., ketones, esters, and carboxylic acid groups. The autoxidation of simple low molecular weight organic compounds is quite well understood, but the oxidation of polymers is much more complex.[6]

An important feature of the aging of thick-walled polymer products is the diffusion-controlled nature of the oxidation. The outer layers of a polymer product are oxidized more than is the interior of the product.[11] The depth of penetration of oxidative aging decreases as the aging temperature is raised. The increase in the rate of oxygen consumption is greater than the increase in the rate of diffusion caused by the higher temperature and less oxygen is available for diffusion within the polymer.[12] Because of the lower permeability of oxygen through the oxidized material,[13,14] the interior of the polymer may actually become destitute on oxygen when an oxidized layer is formed on the polymer surface.[15,16] This means that there will be an essentially anaerobic aging of the interior of the material, and the resistance to aging will be governed by the thermal stability of the material.

In an antioxidant-free material, the oxidation of the surface proceeds rapidly and only small amounts of oxygen are able to diffuse into the bulk material. On the other hand, in stabilized materials, the formation of an oxidized layer, which actually would be capable of preventing diffusion of oxygen into the material, is slow due to the low rate of oxidation. In stabilized materials, oxygen can therefore diffuse into the material and most probably give a deeper oxidation when the antioxidants are depleted by reaction or migration. This paradoxical effect of antioxidants was shown in a previous paper[16] when the thermooxidative aging of natural rubber (NR) was followed using FTIR and computed X-ray tomography scanning. Results from practical applications have been presented, for instance, by Davies,[17] showing that unstabilized rubber materials used for long times, e.g., a bridge bearing pad of NR used for 99 years, are not degraded below the oxidized outer layer. The protection demands, of course, that the oxidized layer be left intact,[18] which excludes most dynamic applications, since an oxidized layer is brittle. However, the protective properties

---

Initiation   a) In the initial stage

$$RH \xrightarrow{\Delta, h\nu, \text{stress}, \gamma, \beta} R\cdot + H\cdot$$

b) Thermal decomposition of hydroperoxides

$$ROOH \longrightarrow RO\cdot + \cdot OH$$
$$2\,ROOH \longrightarrow RO\cdot + RO_2\cdot + H_2O$$

Propagation $R\cdot + O_2 \longrightarrow RO_2\cdot$

$RO_2\cdot + RH \longrightarrow ROOH + R\cdot$

Termination $R\cdot + R\cdot \longrightarrow R-R$

$R\cdot + RO_2\cdot \longrightarrow ROOR$

$RO_2\cdot + RO_2\cdot \longrightarrow$ non-radical products $+ O_2$
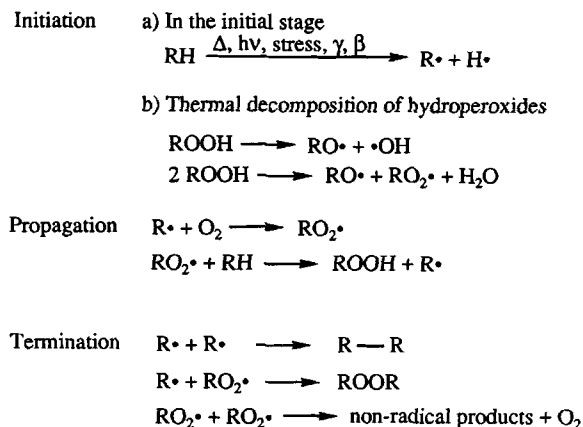
Figure 1 The autoxidation mechanism for hydrocarbon materials.

of an oxidized layer suggest that materials might be made oxidation-resistant by surface-modification techniques. If a proper selection of reactants is made, material surfaces less permeable to oxygen, but still flexible, may be created.

Our first contribution to the surface modification of rubber materials was reported in the mid-1980.[19] A butyl rubber (IIR) coating, known to have a low permeability coefficient for oxygen, was applied to NR cylinders in order to achieve better aging properties. The conclusion reached was that the protection against thermooxidative aging came from the butyl rubber coating and that it worked mainly by stopping the diffusion of oxygen from the surrounding air. The experimental procedure with the IIR-coating was successful, but the technique used was cumbersome and time-consuming. In a recent pa-
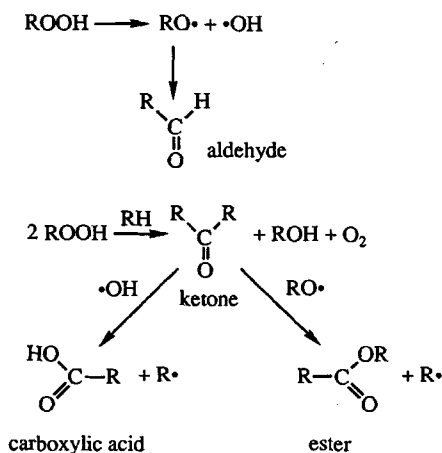
$$ROOH \longrightarrow RO\cdot + \cdot OH$$

Figure 2 Carbonyl structures produced in hydrocarbon autoxidation.

per,[20] we described two more generally applicable modification techniques—plasma polymerization and electron irradiation—with examples of applications in rubber technology. The conclusion reached was that plasma polymerization was the most promising technique. However, the mechanical properties have to be investigated. Plasma polymerization has sometimes been claimed not to affect bulk properties. This is surprising since the heavily cross-linked polymer plasma layers that are often created ought to restrict, e.g., flexibility.

In the present paper, we report the use of plasma polymerization for modification of rubber materials and complementary experiments utilizing a photografting technique. We report on the modification procedures, characterization of structures, and the properties of the surface modifications achieved.

EXPERIMENTAL

Materials

The compositions of the rubber materials used are listed in Table I. For the measurements of oxygen permeability, two layer films of LDPE and EVA, VA content 3% (50 μm thick, 0.922 g/cm^3, corona-treated) were used as a model substance for hydrocarbon rubber materials due to difficulties in making accurate measurements of oxygen permeability on rubber sheets. Permeation occurs in the amorphous phase of a semicrystalline polymer and is therefore less than that in a totally amorphous polymer. It is acceptable to use the LDPE/EVA film as a model substance for rubber materials when estimating the effects of different surface modifications. "Monomers" used for the plasma treatments were C_2F_4, acrylic acid (AA), oxygen, and argon. AA was the monomer used for photografting.

Table I   The Compositions of the Rubber Materials Used

NR	phr	EPDM	phr
SMR5CV	100.0	Vistalon 2504	100.0
Stearic acid	2.0	FEF N550	50.3
ZnO	5.0	Ketjenblack EC	20.0
CBS	1.2	Paraffinic oil	20.5
Sulfur	2.5	ZnO	5.0
		Antilux 654	5.0
		Stearic acid	1.0
		Luperco 500-RC (99% active dicumyl peroxide)	3.2

Plasma Polymerization

Plasma polymerization[21,22] is the formation of a polymer material from a partly ionized "monomer" gas in a glow discharge. This kind of polymerization proceeds via mechanisms totally different from those of conventional polymerization processes and the polymer formed possesses structures and properties different from any other polymer.

The plasma-polymerization process usually starts from a relatively simple gas, generally not considered as a "monomer" for polymerization. In fact, it can be almost any organic (or even some inorganic) molecule.

The desired product of the plasma treatment is a thin film, less than 1 μm thick. This film has a complex structure and is highly cross-linked. The high degree of cross-linking is supposed to impart chemical resistance and low gas diffusion. The main reason for the complex structure is the great number of different reactive species present in the plasma, e.g., ions, radicals, and various excited fragments.

A simplified mechanism for plasma polymerization was proposed by Yasuda.[21] His "rapid step growth model," shown in Figure 3, is valuable for an understanding of plasma-polymerization principles and illustrates the complexity of the processes.

All plasma treatments reported in this paper have been performed at the Institute for Surface Chemistry in Stockholm (YKI). The reactor used is schematically shown in Figure 4. The gas flow rate was fixed at a level equivalent to 10 cm^3/min of nitrogen gas. Different monomers behave differently in a plasma environment. Therefore, appropriate plasma parameters have to be chosen for each monomer gas.[22] Based on experience at YKI, the following parameters were used:
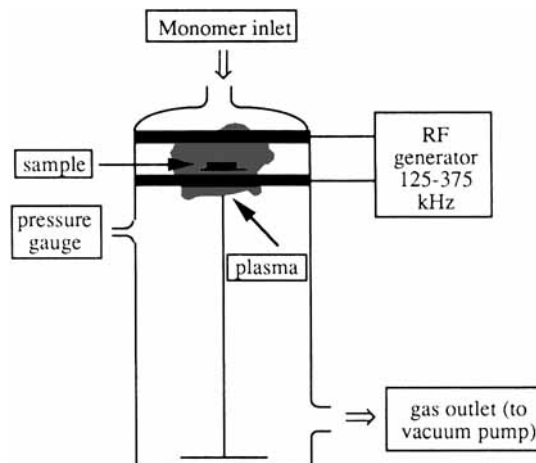

Cycle I: Rapid step-growth by reactivation of reacted products with monofunctional activated species.
Cycle II: Rapid step-growth via multifunctional activated species such as diradicals, ion-radicals etc.

Figure 3 The "rapid step-growth model" showing possible mechanisms in plasma polymerization.

Figure 4 The plasma reactor at YKI.

- For C_2F_4, oxygen, and argon: 5 min treatment time using a power discharge of 50 W. Some additional treatment were made at lower power discharges.

- For acrylic acid: 3 min treatment time using a power discharge of 5 W. Some additional treatments were made at higher-power discharges.

Photografting

Radiation in the near UV is not absorbed by most hydrocarbon polymers but is well absorbed by UV initiators. The initiator most commonly used for grafting is benzophenone or its derivatives. When benzophenone is excited by UV irradiation, it abstracts hydrogen from the polymer matrix, forming a polymer radical. This reactive site then initiates polymerization of the monomer. The reaction is shown in Figure 5. The monomer used for photografting in this study is AA, since it makes it possible to compare the photografting technique with the plasma technique.
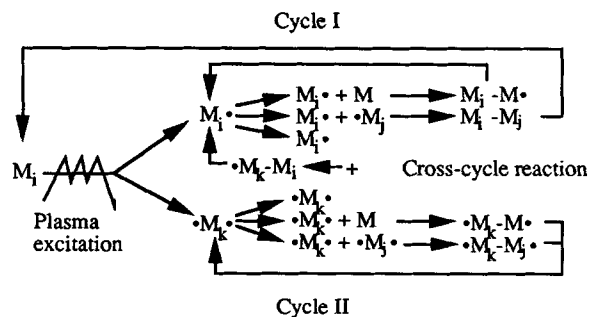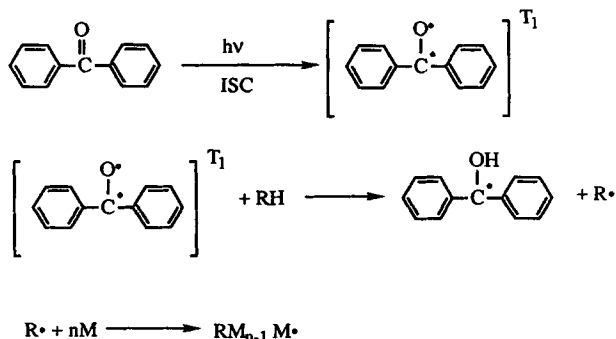

R• + nM ⟶ RM$_{n-1}$ M•

Figure 5 The mechanism for initiation of photografting.

The grafting procedure followed a route described earlier.[23,24] The polymer sample to be grafted was placed in the reactor shown in Figure 6. The small beakers contained $2M$ AA and $0.2M$ benzophenone in acetone. The reactor was purged with nitrogen for 2 min and heated to 55°C. Samples were UV-irradiated for predetermined times through a quartz window. Since monomer and initiator were supplied in the vapor phase, the UV-transparent LDPE/EVA films were automatically grafted on both sides. For the opaque rubber materials, each side had to be treated separately. The grafted materials were washed in acetone, methanol, and water in order to remove reactants and homopolymer formed during the grafting reaction.

ESCA

Electron spectroscopy for chemical analysis (ESCA)[25] is a powerful method for surface characterization. It gives both qualitative and quantitative information on the composition of an approximately 2 nm-thick surface layer. The sample is exposed to X-rays of a specific wavelength. The X-rays detach core electrons from the sample as shown in Figure 7. The energy of the detached electrons, E_{kin}, depends on the binding energy, E_b, of the electron to the core and the energy of the exciting photons, $h\nu$:

$$E_{kin} = h\nu - E_b - \phi,$$

where ϕ is a work factor specific for each system.

Core electrons are not considered to contribute to chemical binding. However, their ionization energies vary somewhat depending on the nature and number of neighboring atoms.[25] The most marked effect is exerted by electronegative atoms,
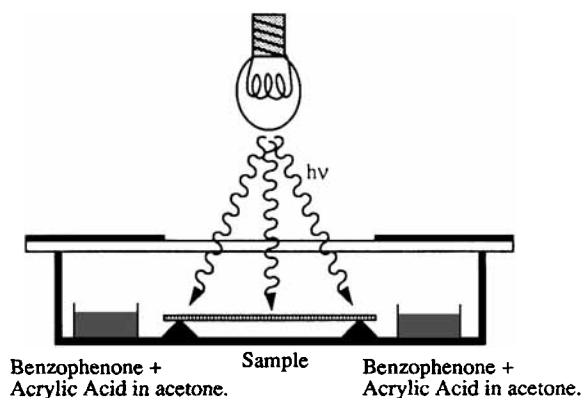

Figure 6 The reactor used for photografting.

Benzophenone +
Acrylic Acid in acetone.

Sample

Benzophenone +
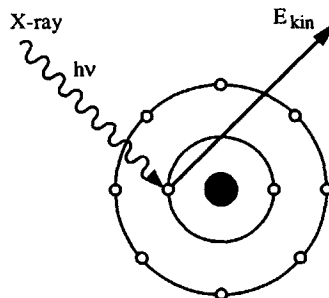Acrylic Acid in acetone.

X-ray

E_{kin}

$h\nu$

Figure 7 A schematic diagram of the ESCA principle.

e.g., F and O, which decrease the shielding of the positive nuclear charges by outer electrons, thus increasing the effective attractive force of the nucleus with regard to the core electrons. An impressive series of papers has been presented by Clark and co-workers regarding ESCA spectra of fluoroplasma polymers.[26-30]

The ESCA spectra were recorded on a Leybold Heraeus ESCA/Auger spectrometer LH 2000, with an AlKα X-ray radiation source. For quantitative analysis, the atomic sensitivity factors (ASF) reported by Briggs and Seah[31] were used: 0.25 for the C1s peak, 0.66 for O1s, and 1.00 for F1s.

Infrared Spectroscopy

IR spectroscopy of polymers is based on the excitation of vibrations by the absorption of photons.[25] The most important selection rule is the change in dipole moment during excitation. Strong IR absorptions are displayed by polar groups, perhaps the best known example being the carbonyl group. Small, but analytically significant, shifts are due to neighboring groups,[32] e.g.:

- Ester, approximately 1740 cm^{-1}.
- Ketone, approximately 1715 cm^{-1}.
- Carboxylic acid, approximately 1700 cm^{-1}.

The low wavenumber for carboxylic acid is due to hydrogen bonding, which decreases flexibility. Transmission IR spectra were recorded using Perkin-Elmer FTIR 1725X.

Contact Angle Measurements

The measurement of the contact angle[33] between a liquid and a polymer is one of the easiest ways to characterize a polymer surface. A liquid is applied to the surface and only the outermost surface layers interact with the liquid. A hydrophobic surface with

low free energy gives a high contact angle with water, whereas a wetting, high-energy surface allows the drop to spread, i.e., gives a low contact angle. The contact angles reported in this paper were measured when the water drop moved over the dry surface, the so-called advancing contact angle.

Swelling

It is possible to estimate the homogeneity of a surface modification by measurement of the swelling of the rubber material in specific solvents. If, for instance, the rubber surface is modified with polar groups, the penetration of nonpolar solvents into the material is retarded and the material swells at a slower rate. However, if the surface is heterogeneously coated, the solvent can penetrate through the uncoated parts. In this work, swelling was measured using ASTM-III oil at room temperature.

Oxygen Permeability

Two mechanisms, leakage and permeation, are responsible for the transmission of oxygen through a polymer. Leakage can occur through pinholes or cracks, i.e., when oxygen passes through a discontinuity in a material or between the surfaces of materials in physical contact. Permeation occurs when oxygen passes through the material itself. Hence, leakage is not dependent upon the type of polymer, but permeation is. The permeation of oxygen through polymers is essentially due to the absorption and solution of oxygen at a polymer surface and to the diffusion of oxygen through the polymer and desorption from the reverse side.

With regard to permeation, a surface-modified material, e.g., a plasma-treated or a heavily oxidized polymer, should be regarded as a composite. The solubility and diffusion in the bulk differ from the properties at the surface. If, however, the rate of oxygen permeation through the material is measured to determine the effect of surface modifications and not to determine specific values of diffusion and solubility coefficients, modified materials may be studied without any special precautions.

Oxygen permeation data reported in this paper were determined using an Oxtran 2/20 MH instrument from Mocon, Minneapolis, MN, earlier described by Demorest[34] and in ASTM standards.[35] The measurements were made at 23°C and with a relative humidity of 50% unless otherwise stated. The oxygen transmission rates, measured by the Mocon instrument, are equal to permeation rates since there is no difference between the partial pressures of oxygen on the two sides of the film. The permeation rate can then be converted into a permeability coefficient by multiplying by the thickness of the film.

Oxidative Stability

Differential scanning calorimetry (Perkin-Elmer DSC-2) was used to measure the oxidative stability of modified materials. The energy flow for NR samples (11 mg) was followed during a temperature scan from 50 to 200°C (5°C per min) in an oxygen atmosphere.

Tensile Modulus

Measurements of tensile modulus were performed isothermally (30°C) at 1 Hz using DMTA (Polymer Laboratories Mk II). The specimens were 160–200 μm thick with a width of 3 mm. The distance between the two sample holders was 3 mm.

Adhesion Measurements

A specially designed computer-controlled instrument, schematically shown in Figure 8, was used to measure the adhesive properties of rubber materials after plasma treatment. The motor (2) applies a force of 0.04 kp (40 pond, approximately equivalent to 40 g) to the sample (4). After 5 min, the force is released at a controlled rate. The weight decrease is followed by the weighing machine (1). If there is good adhesion between the rubber and the metal cylinder (3), the specimen sticks to the metal cylinder and the weighing machine reports a negative weight until the specimen falls from the cylinder.
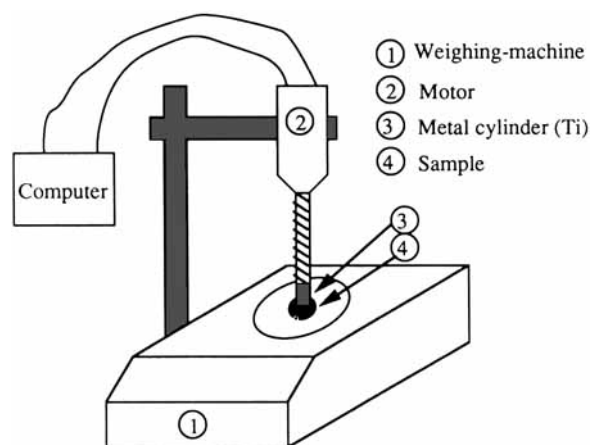

① Weighing-machine
② Motor
③ Metal cylinder (Ti)
④ Sample

Figure 8   The instrument used to estimate rubber/metal adhesion.
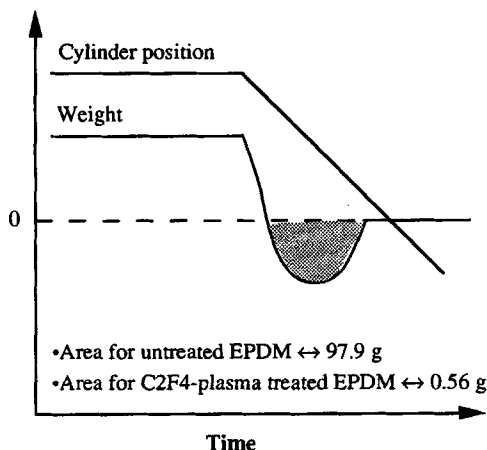
Figure 9   Example of data obtained from the instrument depicted in Figure 8.

The type of diagram obtained is shown schematically in Figure 9. The shaded area, which may be taken as a measure of adhesion, is cut from the plotter paper and weighed.

Friction Measurements

The frictional force opposing motion is proportional to the normal force, the constant of proportionality being the coefficient of friction,[36] i.e.:

$$F = \mu N$$

where F is the frictional force; N, the normal force; and μ, the coefficient of friction. In contrast to most other types of materials, the coefficient for polymer materials should be considered as a "variable constant" since its value is affected by the real contact area, the normal load, the velocity, and several other factors. However, friction measurements may give important qualitative information about surface-modification effects.

Heterogeneities in plasma coatings severely affect the friction measurements. To exclude such heterogeneities that, according to a previous study,[20] may appear near the edges of the polymer substrate, specimens for friction measurements (40 × 40 mm) were cut from larger samples (100 × 100 mm) treated in the plasma reactor. The tests were run using a steel plate at a velocity of 100 mm/min with a normal force of 20 N.

RESULTS AND DISCUSSION

Chemical Characterization

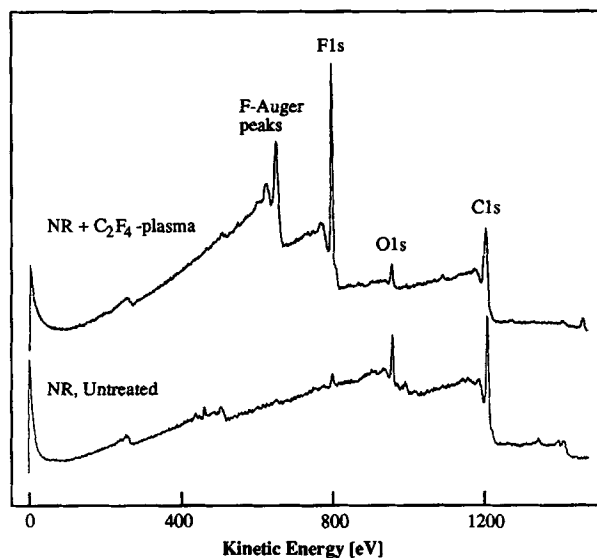ESCA spectra of plasma-treated rubber materials are shown in Figures 10–13. The effective coating

Figure 10   ESCA spectra of untreated NR and NR treated in a 50 W C_2F_4 plasma.

obtained using the C_2F_4 plasma on NR is shown in Figure 10. The C/F value is 1.0 for this treatment. Theoretically, it is expected to be 0.5. The presence of F atoms at the surface of untreated NR is due to a fluoro-containing mold release agent. The structures of the C_2F_4 plasma polymers, which were alike regardless of substrate, are shown using the C1s peak from EPDM (Fig. 11) that was slightly better coated (C/F = 0.80). The peak is shifted toward higher binding energies as expected, i.e., showing C attached to 1, 2, and 3 fluoro atoms. Additional peaks may be explained[27] by shifts caused by structures like $CF - CF_n$.

The results of the plasma treatments using AA as the monomer are shown in Figure 12. As indicated by the C/O values, the coating was relatively poor for both 5 and 50 W. Theoretically, it is supposed to be 1.5. The reason for this poor coating is not
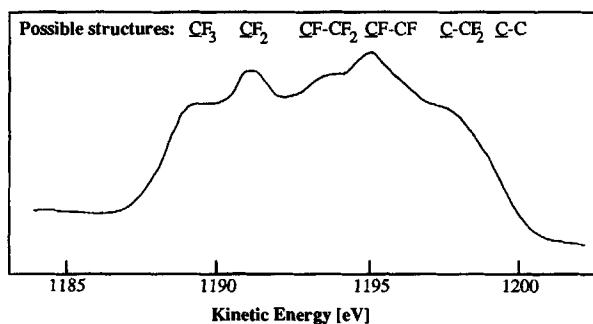

Figure 11   The C1s ESCA peak for EPDM treated in a 50 W C_2F_4 plasma.
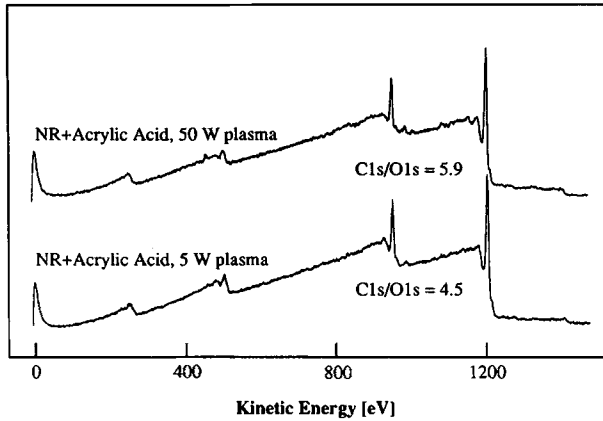
Figure 12   ESCA spectra of NR treated in a 5 W and a 50 W AA plasma.

understood. No dramatic changes in coating efficiency were observed due to the change in power discharge. However, when the C1s peaks were analyzed, differences in the plasma polymer structure were discernible (Fig. 13). The C1s peak for the material treated at 5 W was shifted toward higher binding energies and showed a shoulder. This is explained as being due to a higher content of carboxylic acid groups (three carbon–oxygen bonds) in the surface of materials treated in 5 W plasmas than in those treated at 50 W, which probably is predominated by ketone structures (two carbon–oxygen bonds).

The reason for this difference in chemical structure is ascribed to the degradation of the AA monomer into smaller species at 50 W. The degradation of the acrylic monomer at 50 W is indicated by a pressure increase during the plasma process. At 5 W, the monomer is left rather intact and the poly-
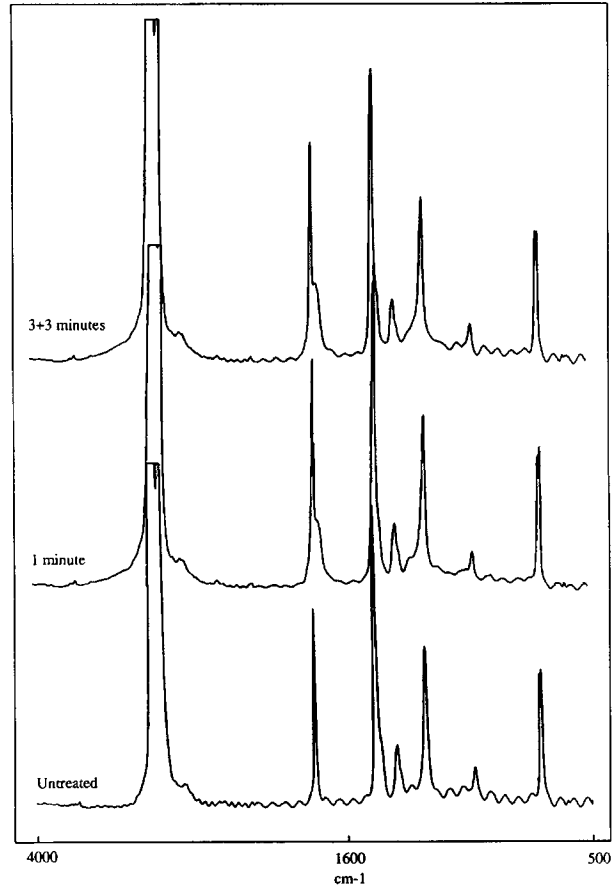

Figure 14   IR spectra of untreated LDPE/EVA and LDPE/EVA UV-irradiated for 1 and 6 min in AA.

merization of AA and the photografting of AA therefore give similar structures. Photografting of AA gave rise to surfaces rich in carboxylic acid groups. This is shown in Figure 14 for a grafted LDPE/EVA substrate. The shoulder to the right of the ketone IR absorption at 1740 cm^{-1} shows the presence of carboxylic acid groups. The high carbonyl absorption in the untreated material is ex-

Figure 13   The C1s ESCA peak for NR treated in a 5 W and a 50 W AA plasma.
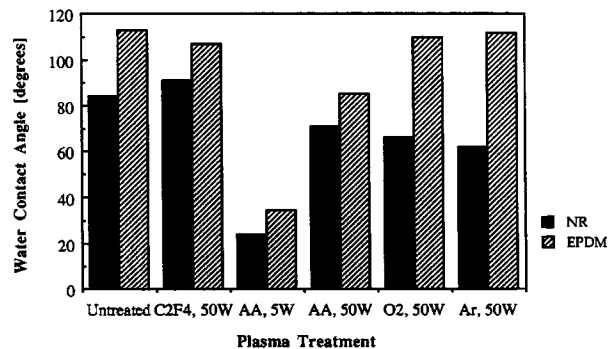

Figure 15   Water contact angles for different treatments of NR and EPDM.

plained as being due to the EVA and the corona treatment.

Contact angles for water on plasma-treated materials are shown in Figure 15. The results corroborate the suggested mechanism regarding plasma reactions. The greater hydrophilicity shown by the surfaces treated at 5 W in an AA plasma is in agreement with the higher content of carboxylic acid groups found there than on surfaces treated in a similar plasma at 50 W.

The high contact angle shown by untreated EPDM is supported by the ESCA data. The C/O value was 48.5, which indicates a very hydrophobic surface. For untreated NR, which was not as hydrophobic as expected, the C/O value was low (C/O = 6.7). This is probably due to oxidation during the manufacture of the NR samples.

Physical and Mechanical Properties

The swelling behavior of NR and EPDM is shown in Figure 16(a) and (b), respectively. Insignificant swelling of the plasma-treated samples was expected since fluorinated rubbers (FPM) and acrylate rubber (ACM) show only little swelling in ASTM-III oil[37]:

- FPM swells 1% by weight after 14 days at 23°C.
- ACM swells 0.4% by weight after 14 days at 23°C.

The unexpected, large swelling found may be due to uncoated regimes present at, e.g., the edges of the specimens.[20] The reason for this uneven coating is not completely understood, but it is known that reactor geometry as well as substrate geometries affect
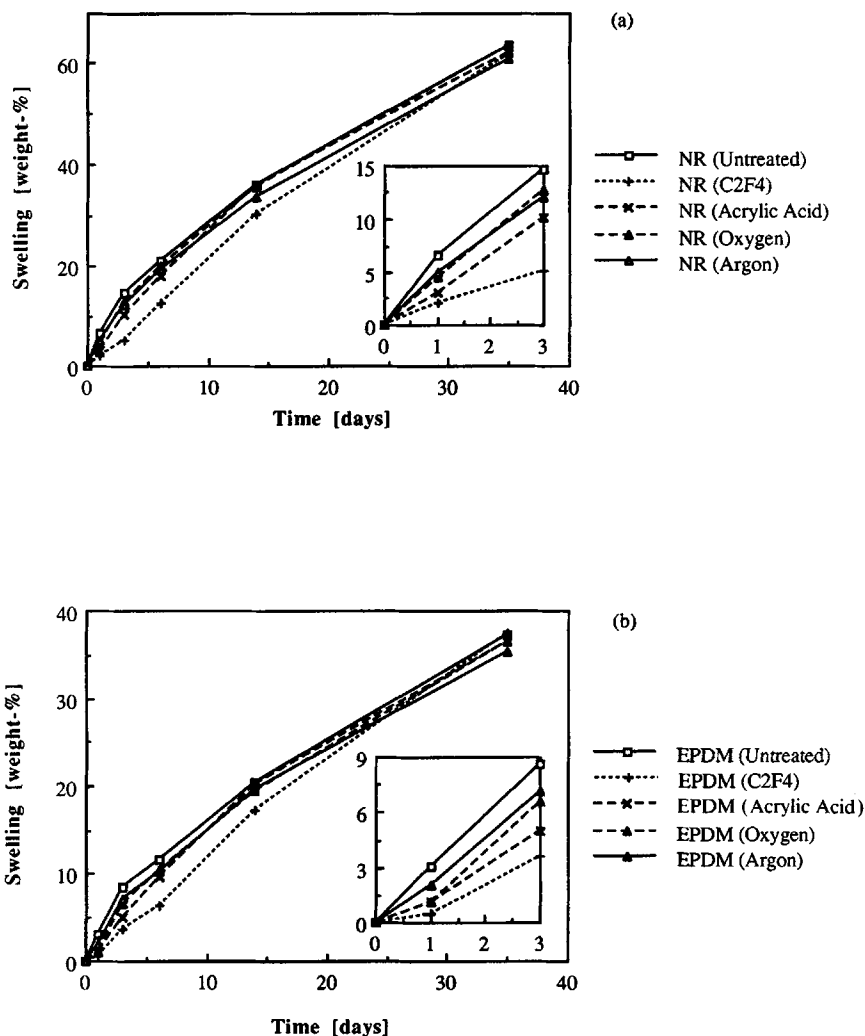

Figure 16   (a) The swelling behavior of NR specimens treated by plasma polymerization. (b) The swelling behavior of EPDM specimens treated by plasma polymerization.

the plasma-polymerization process. The results in Figure 16 may be explained accordingly: Initially, diffusion of oil through the plasma polymer layer is slow, but the diffusion is rapid through uncoated parts of the sample. The oil taken up by the specimen makes it swell and, consequently, the uncoated areas grow. At long times, the swelling thus resembles that of an untreated material. If uneven coating can be avoided, e.g., by a continuous rotation of the sample in the plasma reactor during the treatment, plasma polymerization has the potential to make materials oil-resistant.

The effect of surface modification on permeation of oxygen was studied using LDPE/EVA films
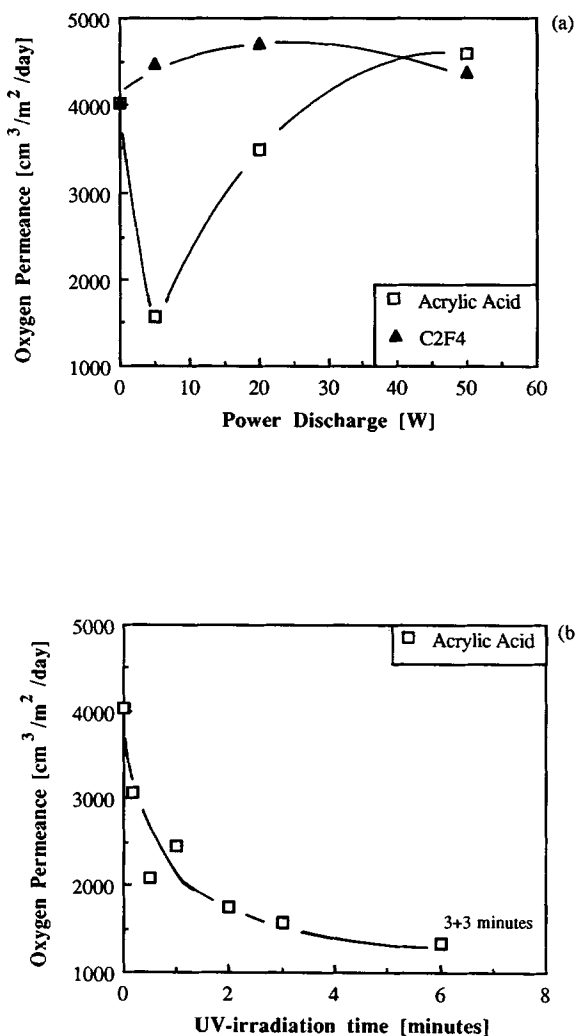
Figure 17 (a) Oxygen permeation rate through LDPE/EVA films treated using plasma polymerization vs. power discharge. (b) Oxygen permeation rate through LDPE/EVA films treated using photografting of AA vs. irradiation time.

(thickness, 50 μm) as a model substance for hydrocarbon rubbers, since it is easier to make accurate measurements on thin plastic films than on rubber sheets. The rate of permeation of oxygen through untreated LDPE/EVA is shown in Figure 17 to be 4027 ($cm^3/cm^2 \times$ day) at 1 atm, which corresponds to a permeability coefficient of 20.1 ($cm^3 \times cm/cm^2 \times$ day $\times$ atm). This is in good agreement with the oxygen permeability coefficient reported for LDPE, 19.3 ($cm^3 \times cm/cm^2 \times$ day $\times$ atm), in the polymer handbook.[38] In the same reference, the oxygen permeability coefficient is reported to be 154 ($cm^3 \times cm/cm^2 \times$ day $\times$ atm) for NR.

The first experimental objective was to clarify whether a highly cross-linked surface is sufficient to reduce the permeation rate of oxygen. If the polymer chains are tightly bound together, they should resist the separation necessary to form a void capable of accommodating a diffusing molecule. Such structural tightness should be found not only in highly cross-linked polymers, but also in those possessing a high degree of crystallinity, symmetry, or strong cohesive forces brought about by polarity.[39] However, the oxygen molecule is small compared to hydrocarbon permeants, e.g., oils, where a "fishing-net-catching" of the permanent can be assumed. It is obvious from Figure 17(a) that a "fishing-net theory" is not relevant for oxygen permeation through plasma polymers, since the permeation through the fluoroplasma-treated sample, which would be a very good candidate for forming such a net, is unchanged compared with that of the unmodified material. On the other hand, Figure 17(a) and (b) show that the permeation decreases through a polymer material when AA is grafted onto the surface, although this is true only if there is a reasonably "clean" grafting polymerization as observed for plasma at 5 W and photografting. When the power discharge was increased to 50 W, the plasma polymerization became very complex and the oxygen permeation even surpassed that of the original uncoated level. The conclusion is that the low permeation obtained by grafting AA to surfaces is due to the content of carboxylic acid groups, thereby inducing a high cohesive energy density. This is in good accordance with data presented by Yasuda,[21] who reports a decrease in oxygen permeability as the cohesive energy increases in the following series of polymers: poly(dimethylsiloxane) < natural rubber < polyethylene < polytrifluorochloroethylene < poly(vinylidene chloride) < polyacrylonitrile.

Figure 18 shows the dependence of permeation on temperature and relative humidity for the material treated in a 5 W AA plasma. The behavior
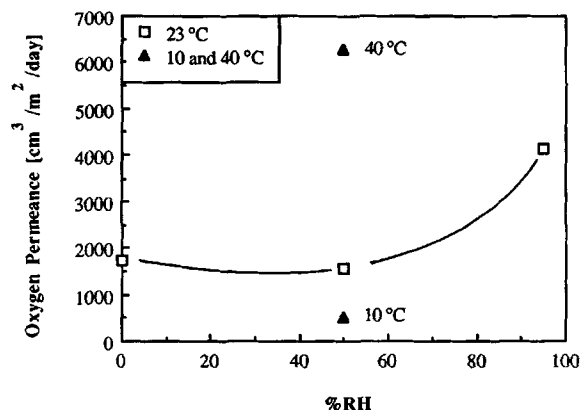
Figure 18 The dependence of oxygen permeation rate on temperature and relative humidity for LDPE/EVA treated in a 5 W AA plasma.

Figure 19 Oxygen permeation rate through LDPE/ EVA films aged at 60°C in an Atlas UVCON "weatherometer."

shown by this material is similar to that of EVOH, which often is used in the packaging industry because of its superior oxygen barrier properties. However, when the humidity is high, the barrier properties are lost, probably due to the plasticizing effect of the sorbed water creating a looser polymer network, which makes it easier for voids to be formed, to accommodate the permeant. Since a high humidity also interferes and disrupts the hydrogen-bonded structures[40] in the surface of the sample treated in an 5 W AA plasma, the barrier properties are susceptible to high humidities.

The high permeability of the fluoroplasma-treated film, indicating no correlation between dense networks and oxygen permeability, conflicts with the behavior of the hydrogen-bonded 5 W AA plasma-treated surface and the photografted surface, which indicates that linkages resisting separation afford enhanced barrier properties. This contradiction indicates that, besides the restricted mobility afforded by cross-linking, crystallites, or strong cohesive forces, certain chemical functionalities also influence the permeation. To clarify this, more research efforts are required.

Permeation of oxygen decreases during thermooxidative aging. This is shown in Figure 19 for LDPE/EVA films aged up to 400 h in an Atlas UVCON "weatherometer" at 60°C. The IR spectra for corresponding materials are displayed in Figure 20. These spectra are in good accordance with the mechanisms given in Figure 2, suggesting that carboxylic acid and ester groups are two major functionalities formed in thermooxidative degradation. In this article it has been shown that a surface treated with a 50 W AA plasma probably contains ketone structures, which apparently do not affect
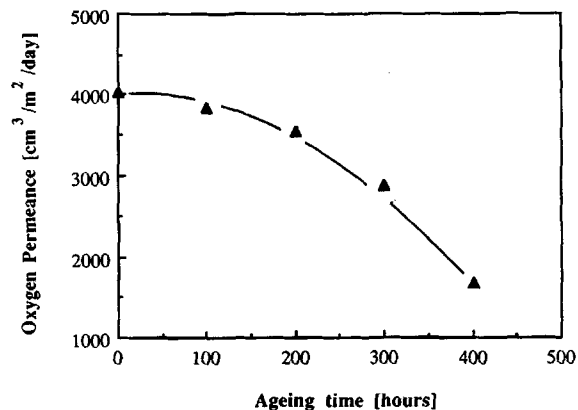
the permeation of oxygen. This is supported by the permeation rate through the "untreated" LDPE/ EVA film, which is in good accordance with the literature data, although the LDPE/EVA film in the present study has a high carbonyl absorption, due
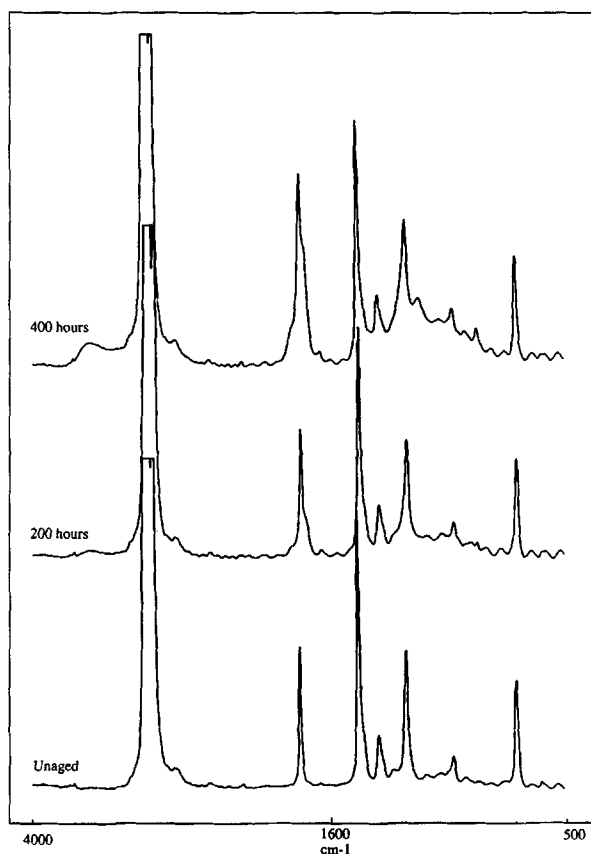

Figure 20 IR spectra of untreated LDPE/EVA and LDPE/EVA aged 200 and 400 h at 60°C in an Atlas UVCON "weatherometer."
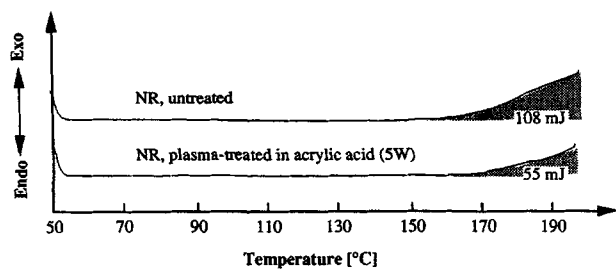
Figure 21 A DSC thermogram showing the exothermal oxidation peaks for untreated NR and NR treated in a 5 W AA plasma.

Figure 23   Tensile modulus for surface-modified NR specimens.

to the EVA and the corona treatment. In contrast, the photografting of AA or plasma treatment in a 5 W AA plasma affords surfaces with a high content of carboxylic acid groups that decrease the permeation of oxygen. It is thus obvious that carboxylic acid groups with their hydrogen-bonding capacity play a very important role in the diffusion-limited oxidation.

To ensure that a decrease in permeation results in an increase in oxidative stability, the oxidative exothermal peak in a DSC temperature scan was measured. As shown in Figure 21, there is an increase in the oxidative stability after 5 W AA plasma treatment, i.e., a smaller exothermal peak is recorded. There is also an increase in oxidative stability after the fluoroplasma treatment (Fig. 22). Since there is no decrease in permeability in this case [Fig. 17(a)], this increase in oxidative stability is probably because fluorinated polymer structures are more stable than are simple hydrocarbons. The problem of achieving a homogeneous coating using plasma polymerization probably becomes more pronounced in the case of small samples with a high ratio of edge
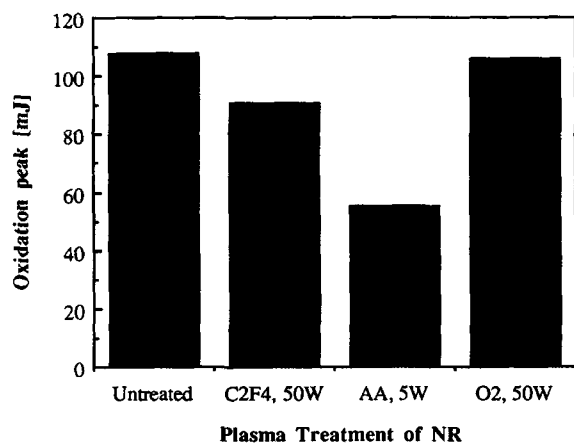
area to surface area. For specimens used in the oxidative stability measurements, the uneven coating effect was not detectable, probably because of the small thickness, less than 1 mm, of these specimens.

The tensile modulus for surface-modified rubber materials is shown in Figure 23. Although scattering is large between measurements (six specimens from each treatment), it is obvious that there is an increase in modulus for the plasma-treated material as well as for the photografted materials. The increase is in the range of 10–20%. This "bulk effect" must not be neglected if rubber products for high elasticity applications are surface-modified.

Plasma treatments using fluoromonomers decrease the adhesion between rubber and metals, as shown in the plot in Figure 9. The adhesion between a C_2F_4-treated EPDM and a metal cylinder decreases by a factor of nearly 200 compared with the adhesion

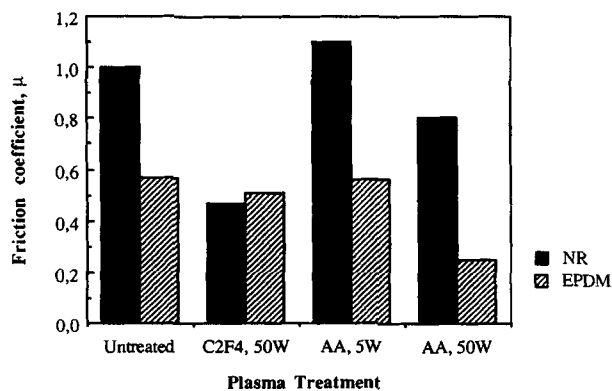**Figure 22**   The exothermal oxidation peaks, determined as in Figure 21, for different treatments of NR.

Figure 24   The coefficient of friction, μ, shown by the treated materials.

of untreated material. This may be interesting in applications where a very high abrasion resistance of the elastomer is required.

The results of the friction measurements are shown in Figure 24. It is obvious that a C_2F_4 plasma polymer surface shows a lower friction coefficient, although a more pronounced reduction was expected for the EPDM specimen according to the adhesion test results. This may be explained as being due to some contamination on the surface prior to or during the test. It is surprising that the treatment in a 50 W AA plasma gave such a low coefficient of friction compared with that of the 5 W AA plasma treatment. This may be related to the differences in surface structure indicated by the contact angle measurements. It is of interest to note the "slip-stick" effect, i.e. the coefficient of friction between the two surfaces oscillates about a mean value. The "slip-stick" effect is much stronger for the materials showing high friction, i.e., untreated samples and samples treated in a 5 W AA plasma. For these materials, the "slip-stick" amplitude is greater than 50% of the mean value reported in the figure. For treatment using C_2F_4 and AA at 50 W, the amplitude never exceeds 10% of the mean value. The "slip-stick" effect is due to a buildup of force as in a spring during the time the surfaces stick together. When the force exceeds a certain value, the spring releases and the cycle is repeated. The "slip-stick" effect indicates that the differences in frictional properties are probably even more pronounced than is indicated by Figure 24.

CONCLUSIONS

Surface modification of rubber materials is a promising technique to achieve stabilization. Utilizing acrylic acid (AA) as the monomer, both plasma polymerization and photografting prove to be suitable techniques to obtain surfaces with low oxygen permeation rates. Because of the barrier properties toward oxygen, these materials possess increased oxidative stability. The results presented are in good accordance with theories of diffusion-limited oxidation of thick-walled materials discussed in previous papers. During aging, carbonyl groups are produced in the surface layer and the permeability to oxygen decreases. However, an oxidized layer of this kind is brittle and will crack in flexible applications. The surface modifications using AA reported in this article decrease the permeation but retain a great deal of flexibility. The decrease in oxygen permeation shown by surfaces modified using

AA indicates an important role of carboxylic acid groups, with high cohesive energy densities and the ability to hydrogen bond.

Surface modification changes other properties as well. The materials treated in an AA plasma or in a fluoroplasma showed reduced swelling rates, but due to uneven coating, the oil-resistance was not as good as expected. Modifications using fluoromonomers do not affect oxygen permeation properties, but the adhesion to metals is strongly reduced and the coefficient of friction is lowered. A decrease in friction was observed for samples treated in an AA plasma at 50 W but not when the power discharge was lowered to 5 W.

The increase in tensile modulus determined for surface-modified rubber materials must be considered when applications for the presented techniques are discussed.

REFERENCES

1. S. J. Weininger and F. R. Stermitz, Organic Chemistry, Academic Press, Orlando, FL, 1984, Chap. 5.
2. F. A. Carey and R. J. Sundberg, Advanced Organic Chemistry, Part B, Plenum Press, New York, 1983, Chap. 10.
3. R. W. Lenz, Organic Chemistry of High Polymers, Wiley-Interscience, New York, 1967.
4. L. Reich and S. S. Stivala, Autoxidation of Hydrocarbons and Polyolefins, Marcel Dekker, New York, 1969.
5. N. C. Billingham and P. D. Calvert, in Developments in Polymer Stabilization—3, G. Scott, Ed., Applied Science, London, 1980, Chap. 5.
6. Y. Kamiya and E. Niki, in Aspects of Degradation and Stabilization of Polymers, H. H. G. Jellinek, Ed., Elsevier, Amsterdam, 1978, Chap. 3.
7. J. R. Shelton, Rubber Chem. Technol., 56, G71 (1983).
8. J. A. Brydson, Rubber Chemistry, Applied Science, Essex, 1978, Chap. 9.
9. M. E. Abu-Zeid, Y. A. Youssef, and F. A. Abdul-Rasoul, J. Appl. Polym. Sci., 32, 3345 (1986).
10. G. Geuskens and M. S. Kabamba, Polym. Deg. Stab., 4, 69 (1982).

11. J. Y. Moisan, in *Polymer Permeability*, J. Comyn, Ed., Elsevier, Essex, 1985, Chap. 4.
12. D. Barnard and P. M. Lewis, in *Natural Rubber Science and Technology*, A. D. Roberts, Ed., Oxford University Press, New York, 1988, Chap. 13.
13. B. Stenberg, Y. J. Shur, and J. F. Jansson, *J. Appl. Polym. Sci.*, **35**, 511 (1979).
14. R. L. Clough and K. T. Gillen, *Polym. Deg. Stab.*, **38**, 47 (1992).
15. R. L. Clough and K. T. Gillen, *Polym. Mater. Sci. Eng.*, **58**, 209 (1988).
16. B. Mattson, E. Östman, S. Persson, and B. Stenberg, *Rubber Chem. Technol.*, **63**, 23 (1990).
17. B. Davies, *Rubber Dev.*, **41**(4), (1988).
18. F. Björk and B. Stenberg, *Polym. Test.*, **5**, 245 (1985).
19. B. Stenberg, L. O. Peterson, P. Flink, and F. Björk, *Rubber Chem. Technol.*, **59**, 70 (1986).
20. B. Mattson and B. Stenberg, *Kautsch. Gummi Kunst.*, **2**, 116 (1992).
21. H. Yasuda, *Plasma Polymerization*, Academic Press, Orlando, FL, (1985).
22. H. V. Boenig, *Fundamentals of Plasma Chemistry and Technology*, Technomic Publ. Co., Lancaster (1988).
23. B. Rånby, Z. M. Gao, A. Hult, and P. Y. Zhang, ACS Symposium Series 364, American Chemical Society, Washington, DC, 1988, Chap. 13, p. 168.
24. K. Allmér, A. Hult, and B. Rånby, *J. Polym. Sci. Polym. Chem.*, **26**, 2099 (1988).
25. W. Klöpffer, *Introduction to Polymer Spectroscopy*, Springer-Verlag, Berlin, Heidelberg, 1984.
26. D. T. Clark and D. Shuttleworth, *J. Polym. Sci. Polym. Chem.*, **16**, 1093 (1978).
27. D. T. Clark and D. Shuttleworth, *J. Polym. Sci. Polym. Chem.*, **18**, 27 (1980).
28. D. T. Clark and D. Shuttleworth, *J. Polym. Sci. Polym. Chem.*, **18**, 407 (1980).
29. D. T. Clark and M. Z. Abrahman, *J. Polym. Sci. Polym. Chem.*, **19**, 2129 (1981).
30. D. T. Clark and M. Z. Abrahman, *J. Polym. Sci. Polym. Chem.*, **20**, 691 (1982).
31. D. Briggs and M. P. Seah, *Practical Surface Analysis by Auger and X-ray Photoelectron Spectroscopy*, Wiley, New York, 1983, p. 511.
32. E. Pretsch, T. Clerc, J. Seibl, and W. Simon, *Tabellen zur Strukturau f klärung organischer Verbindungen mit Spektroskopischen Methoden*, Springer-Verlag, Berlin, 1986.
33. J. D. Andrade, L. M. Smith, and D. E. Gregonis, *Surface and Interfacial Aspects of Biomedical Polymers*, J. D. Andrade, Ed., Plenum Press, New York, 1985, Vol. 1, p. 249.
34. R. L. Demorest, *J. Pack. Technol.*, **Oct.** (1989).
35. ASTM-standard D 3985-81 (1981).
36. R. P. Brown, in *Physical Testing of Rubbers*, Applied Science, London, 1979, Chap. 10.
37. *Rubber, Influence of Organic Liquids on Rubber Materials*, SIS Handbook 131, Affärstryckeriet, Norrtälje, 1976.
38. J. Brandup and E. H. Immergut, in *Polymer Handbook*, Wiley, New York, 1989, Chap. 6.
39. M. T. Goosey, in *Polymer Permeability*, J. Comyn, Ed., Elsevier, Essex, 1985, Chap. 8.
40. T. D. Krizan, J. C. Coburn, and P. S. Blatz, in *Barrier Polymers and Structures*, W. J. Koros, Ed., ACS Symposium Series 423, American Chemical Society, Washington, DC, 1990, Chap. 5.